Intermittent Dissipation at Kinetic Scales in Collisionless Plasma Turbulence

M. Wan,[1] W. H. Matthaeus,[1] H. Karimabadi,[2,3] V. Roytershteyn,[3] M. Shay,[1] P. Wu,[1] W. Daughton,[4] B. Loring,[5] and S. C. Chapman[6]

[1]*Bartol Research Institute and Department of Physics and Astronomy, University of Delaware, Newark, Delaware 19716, USA*
[2]*University of California San Diego, La Jolla, California 92093, USA*
[3]*SciberQuest, Inc., Del Mar, California 92014, USA*
[4]*Los Alamos National Laboratory, Los Alamos, New Mexico 87545, USA*
[5]*Lawrence Berkeley National Laboratory, Berkeley, California 94720, USA*
[6]*Centre for Fusion, Space and Astrophysics, University of Warwick, Coventry CV47AL, United Kingdom*

(Received 17 August 2012; published 5 November 2012)

High resolution kinetic simulations of collisionless plasma driven by shear show the development of turbulence characterized by dynamic coherent sheetlike current density structures spanning a range of scales down to electron scales. We present evidence that these structures are sites for heating and dissipation, and that stronger current structures signify higher dissipation rates. Evidently, kinetic scale plasma, like magnetohydrodynamics, becomes intermittent due to current sheet formation, leading to the expectation that heating and dissipation in astrophysical and space plasmas may be highly nonuniform and patchy.

DOI: 10.1103/PhysRevLett.109.195001 PACS numbers: 94.05.Lk, 52.50.−b, 95.30.Qd, 96.50.Ci

Kinetic plasma dynamics and associated dissipation are often described by waves and instabilities [1–4]. However, observations of solar wind, coronal, magnetospheric and interstellar fluctuations suggest that a description in terms of turbulence and cascade may be appropriate [5–7]. Indeed, magnetohydrodynamics (MHD) simulations in various approximations reveal that a broadband cascade to smaller scales invariably occurs, either through instability [8] or direct couplings [9] unless fluctuations are eliminated or controlled. When several decades of scales are available, the dynamics can approach a self-similar ''inertial range'' state that is terminated by viscous dissipation at small scales. However, for a collisionless plasma, a closed-form dissipation function is not known, and the question becomes what physical processes terminate the inertial range, and convert cascading energy into heat. This issue is crucial for problems such as the heating of the solar corona and the origin of the solar wind [5]. Recently we showed, using state of the art kinetic simulations [10], that a hierarchy of electric current density structures is formed in a kinetic cascade, ranging from ion to electron scales; here we find that reasonable measures of plasma dissipation have a strong quantitative association with these structures. This demonstrates that kinetic plasma dissipation can be intermittent, so that in turbulent space plasmas, heating and dissipation might also be expected to be highly inhomogeneous and patchy [11–13].

This nature of collisionless dissipation has been hotly debated in recent years, with alternative ideas posed in terms of various wave modes, such as kinetic Alfvén waves, whistlers, linear Vlasov instabilities, cyclotron resonance, and Landau damping, to name a few [3–6,14,15]. Many of these approaches tacitly assume that the plasma remains close to a simple perturbed equilibrium. The turbulent cascade scenario differs in important ways: First, smaller scale behavior is driven by larger scale dynamics, and response times decreasing with decreasing scale. The system remains far from equilibrium even if it may be in a statistically steady state. Second, most known types of turbulence produce small scale structures and very nonuniform dissipation. Local enhancements of dissipation are related to local nonlinear stresses that give rise to strong gradients, non-Gaussian statistics, and the phenomenon of intermittency. For fluids, these relationships are embodied in the Kolmogorov refined similarity hypothesis (KRSH) [16,17] which relates fluctuation increments to hot-spots of dissipation. Though unproven, KRSH forms the basis for much of modern hydrodynamic turbulence theory. Although well accepted in hydrodynamics, the KRSH has not been demonstrated, or even precisely formulated, for a collisionless plasma, as far as we are aware. However, the prospect that local coherent structures may be related to dissipation is an intriguing and testable hypothesis that contrasts the classical plasma view of homogeneous dissipation.

The solar wind is a good example of the current lack of closure regarding collisionless plasma dissipation. It is well known that the corona must be heated for the observed wind to exist, and that the measured solar wind radial temperature profile is inconsistent with adiabatic expansion [18]. Sufficient energy is present in fluctuations and velocity stream shears to account for this heating (see Ref. [19] and references therein). It is thus tempting to conclude that the observed MHD cascade connects the large scale energy reservoirs to kinetic scales where thermalization occurs. Indeed the (approximately) Kolmogorov-like power-law fluctuation spectrum spanning more than three decades of scale (from $\sim 10^6$ to $\sim 10^3$ km at 1AU) is often

viewed as the "smoking gun" of energy transfer across scales. The rate of energy transfer ϵ may be estimated from a von Kármán–Howarth analysis as $\epsilon \sim U^3/L$ for fluctuation velocity U and turbulence coherence scale L, or more rigorously from the MHD generalization of the famous Kolmogorov third-order law [20–22]. Remarkably, these two results compare well with the heating required to account for the observed radial temperature gradients [7], which is on average $\epsilon \approx 10^3$ J/kg s [22] at 1 AU. The physical mechanisms for the conversion of cascade into heat remain an elusive and controversial subject. The results presented here add detail to this picture of cascade and kinetic dissipation, and support a strong connection between of heating and coherent structures.

The two-dimensional (2D) simulations solve the Vlasov-Maxwell system of equations using the kinetic particle-in-cell code VPIC [23]. The approach is to drive small scale turbulence using large scale velocity shear. After a startup transient period [10], a strong cascade becomes apparent, and we examine quantitatively the putative connection between structures and dissipation. Only this strong turbulence epoch, and not the instability leading to it, is viewed as relevant to solar wind heating.

The initial density n_0 and magnetic field $\mathbf{B} = B_0[\mathbf{e}_y \sin\theta + \mathbf{e}_z \cos\theta]$ are uniform and distribution function for each species is a drifting Maxwellian with uniform temperature T and drift speed $\mathbf{U} = U_0 \tanh(x/L_V)\mathbf{e}_y$. Here, L_V is the shear layer half-thickness and U_0 is the shear velocity. Periodic boundary conditions are imposed in y; the boundaries at $x = 0$ and $x = L_x$ are conducting for electromagnetic field and reflecting for particles. Results shown here are from a 2D simulation with plasma $\beta = 0.1$, $L_V = 4d_i$, $m_i/m_e = 100$, $\theta = 2.86^o$, and $U_0 \approx 10V_A^*$, and $\omega_{pe}/\omega_{ce} = 2$ where $\omega_{ce} = eB_o/(m_e c)$ and $\omega_{pe}^2 = 4\pi n_0 e^2/m_e$. The initial electron and ion temperatures are equal $T_i = T_e = T$, $d_s = c/\omega_{ps}$ is the inertial length of species s with mass m_s, and $V_A^* = B_0 \sin(\theta)/\sqrt{4\pi n_0 m_i}$. It was performed in a rectangular domain in an x-y plane of size $L_x \times L_y = (50 \times 100)d_i$ and utilized a uniform computational grid with 8192×16384 cells corresponding to cell size of approximately 0.77 Debye length (λ_D). The simulation used 150 particles of each species per cell and $\sim 4 \times 10^{10}$ total particles. We normalize time to $\omega_{ci} = eB_0/(m_i c)$. The characteristic time for attaining the nonlinear phase, related to growth of the Kelvin-Helmholtz mode [10], is $t\Omega_{ci} \sim 80 - 160$. Here we focus on the state of the strong turbulence seen at $t = 507\Omega_{ci}^{-1}$.

A novel feature of this analysis is reduction of noise inherent in the particle-in-cell plasma algorithm through low pass Fourier filtering of the magnetic and electric field at a wave number of about $5d_e^{-1}$. Figure 1 shows the how and why the filter is adopted; later, in Fig. 4, we show how it improves the results. All analyses in this Letter employ the low-pass filtered data.

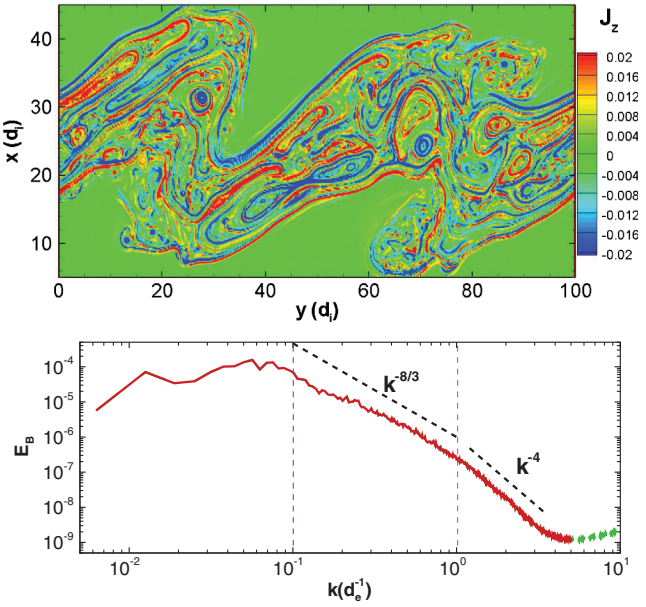

FIG. 1 (color). (Top) contour of z component of current density J_z; (bottom) energy spectrum of magnetic field at $t = 507\Omega_{ci}^{-1}$, dashed line showing signal eliminated by low pass filter cutoff at $kd_e = 5$.

The initial laminar state [10] has become complex by $t\Omega_{ci} = 507$, as shown in Fig. 1: A hierarchy of current structures is visible, spanning a substantial range of size [10]. The sheetlike and eddylike shapes are suggestive of the nonlinear vorticity evolution that is driving the dynamics. The emergence of a broadband spectrum supports this interpretation. Figure 1 also shows the wave number space perspective: At the kinetic scales $kd_i > 1 > kd_e$, the spectrum compares favorably with spectra ($k^{-8/3}$) often reported in this range for samples of solar wind data [4,24–26]. At smaller scales $kd_e > 1$ the spectrum steepens further, also consistent with solar wind observations. A well-defined fluid-scale inertial range is not yet formed [10]. We now turn to a description of the associated intermittency properties.

Intermittency is typically related to coherent structures, which in in fluids are important contributors to dissipation [16,17,27]. It is also established that MHD produces an intermittent fluid-scale cascade [11–13]. Coherent magnetic structures are observed in the solar wind, and the stronger of such "discontinuities" are correlated with locally elevated temperatures [28]. Lacking so far is a quantitative demonstration that a fully kinetic dynamical plasma model produces structures [10], that are associated with strong dissipation. We now provide direct evidence for these connections.

Figure 2 shows a magnified section from Fig. 1, emphasizing the filamentary nature of the electric current density $\mathbf{J} = q(n_i \mathbf{v}_i - n_e \mathbf{v}_e)$ [unit charge, q; proton (electron) number density n_i (n_e); fluid velocity $\mathbf{v}_i$ ($\mathbf{v}_e$)]. To identify regions that might contain elevated dissipation, we have

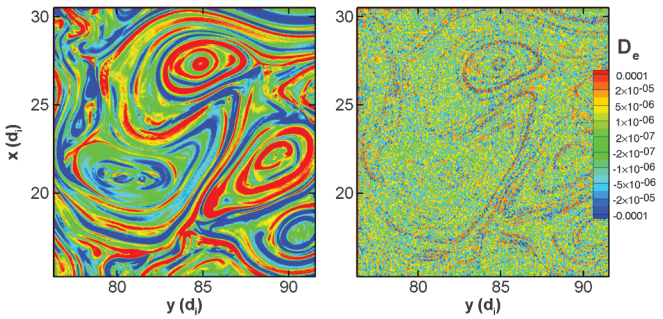

FIG. 2 (color). (Left) J_z in a close-up region of the simulation domain showing hierarchy of coherent structures; (right) Contour of electron-frame dissipation D_e for the region shown in left.

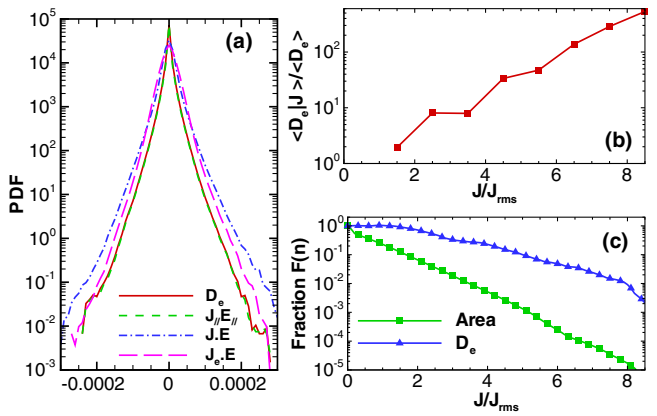

FIG. 3 (color online). (a) PDFs of four dissipation proxies: the electron frame dissipation measure D_e, the laboratory frame D, the parallel dissipation $D_{\|}$, and $\mathbf{J}_e \cdot \mathbf{E}$. (b) Conditional average of dissipation calculated conditioning on the value of current density. (c) Fraction of area (green squares) of the simulation domain where the normalized current density $J/J_{\rm rms}$ is larger than some value n, where $J_{\rm rms}$ is the rms value of J. Also shown is the fraction of dissipation (blue triangles) contributed to the total dissipation from those corresponding areas.

studied $D = \mathbf{J} \cdot \mathbf{E}$, the work done by electromagnetic fields on the particles, in several frames of reference as well as the work on electrons $\mathbf{J}_e \cdot \mathbf{E}$. Conversion of magnetic energy into random kinetic energy must be contained in D, and since particles in collisionless plasmas interact only through the electromagnetic fields, dissipation must be contained in these measures. This identification is complicated by contributions from fluid motions, compressions, particle energization, and reversible motions such as plasma oscillations. To reduce (but not eliminate) contributions due to fluid motions, we may evaluate D in a frame moving with either $\mathbf{v}_e$, or $\mathbf{v}_i$. However, assuming $n_i = n_e = n$, in the proton frame, $D \rightarrow \mathbf{J} \cdot (\mathbf{E} + \mathbf{v_i} \times \mathbf{B}) = \mathbf{J} \cdot \mathbf{E} - qn\mathbf{v}_e \cdot (\mathbf{v_i} \times \mathbf{B})$, while in the electron frame, $D \rightarrow \mathbf{J} \cdot (\mathbf{E} + \mathbf{v_e} \times \mathbf{B}) = \mathbf{J} \cdot \mathbf{E} + qn\mathbf{v}_i \cdot (\mathbf{v_e} \times \mathbf{B})$. Therefore, when $n_i = n_e$, the correction to D due to fluid motion is the same in either frame. To account for the (small) charge separation $\rho_e = q(n_i - n_e)$, we add a correction, for the electron frame, $\rho_e \mathbf{v_e} \cdot \mathbf{E}$. This useful but approximate measure of dissipation (see Ref. [29]) is,

$$D_e = \mathbf{j} \cdot (\mathbf{E} + \mathbf{v}_e \times \mathbf{B}) - \rho_e (\mathbf{v}_e \cdot \mathbf{E}), \qquad (1)$$

which is evaluated for the *local* $\mathbf{v}_e$. A related interpretation of De is the work done by the *nonideal* part of the electric field in a generalized Ohm's law, corrected by removing the work associated with transport of the net charge. D_e is spatially organized in structures that resemble the electric current structures (Fig. 2) providing qualitative evidence of inhomogeneous dissipation. We now turn to quantitative measures.

Figure 3(a) shows the probability density function (PDF) of four dissipation proxies: D_e (as above), the laboratory frame $D = \mathbf{J} \cdot \mathbf{E}$, the "parallel dissipation" $D_{\|} = (\mathbf{J} \cdot \mathbf{B})(\mathbf{E} \cdot \mathbf{B})/|\mathbf{B}|^2$, and the contribution of electron current $\mathbf{J}_e \cdot \mathbf{E}$. The exact electromagnetic dissipation is contained within D and D_e, but these quantities also contain other effects. $D_{\|}$ and $\mathbf{J}_e \cdot \mathbf{E}$ concentrate on the parallel electric field and electron heating [10]. Each proxy has a broad and slightly asymmetric PDF. D has the broadest distribution, as it includes fluid scale stresses that exchange magnetic and flow energies. D_e and $D_{\|}$ do not contain the full fluid contributions and are almost identically distributed. Evidently most dissipation is parallel dissipation. On the other hand a proxy such as $\mathbf{J}_e \cdot \mathbf{E}$ is directly related to the change of electron energy, and therefore includes electron dissipation, but does not separate out changes associated with electron flow.

The slight preponderance of positive values in the distributions (see Fig. 3) produce good agreement of global average values $\langle D_e \rangle = 5.78 \times 10^{-8} c^3/d_e$, $\langle D_{\|} \rangle = 5.81 \times 10^{-8} c^3/d_e$, and $\langle \mathbf{J}_e \cdot \mathbf{E} \rangle = 5.09 \times 10^{-8} c^3/d_e$. We suggest that these are reasonable (but imperfect) estimates of net dissipation of fluid scale energy into plasma internal energy. On the other hand, $\mathbf{J} \cdot \mathbf{E}$ includes large contributions from convective electric field, has a negative average value, and is not an appropriate measure of dissipation.

To better understand the ramifications of a highly structured dissipation, we compute statistics. Figure 3(b) shows averages of D_e conditioned on the normalized local current density, $\langle D_e | J \rangle / \langle D_e \rangle$. The conditionally averaged D_e per unit volume is found to be a strongly increasing function of electric current density. For example, in regions with $J > 8J_{\rm rms}$ the dissipation per unit volume is more than 500 times the global average. However, these regions are rare, occupying less than 0.01% of the volume.

A related question is what fraction of global dissipation measure is found in regions in which the $|\mathbf{J}|$ exceeds a given threshold? Let us define a filling fraction $F(f|n) = \sum' f / \sum f$ where $\sum'$ includes only points where $J/J_{\rm rms} > n$. In Fig. 3(c), we plot the filling fraction for area and for D_e. These diagnostics show that regions of stronger electric current density occupy smaller areas, but make

disproportionate contributions to total dissipation measure. For example, about 70% of the dissipation is found in regions with $J > 2.0J_{\rm rms}$ even though these regions occupy less than 7% of the volume. The alternative dissipation measures $D_{\|}$ and $\mathbf{J}_e \cdot \mathbf{E}$ [see Fig. 3(a)] also have conditional averages (not shown) qualitatively very similar to those of D_e—concentration into small sheet-like regions associated with large values of electric current density.

The global rate of energy decay may be estimated in three distinct ways. First, by directly computing the change in time of fluctuation energy [10], we estimate the dissipation rate as $\Delta E_{\rm fluid}/\Delta t$ for a suitably chosen period of time [10]. We choose the time period $\Delta t = 507\Omega_{ci}^{-1} - 220\Omega_{ci}^{-1}$, and the corresponding fluid scale energy change as $\Delta E = 6.8 \times 10^{-3} c^3/d_e$ during which time the turbulence is fully developed. This estimate gives an average dissipation rate of $1.2 \times 10^{-9} c^3/d_e$, in units of energy per unit mass per unit time. A simple Taylor–von Kármán turbulence decay rate $\alpha(\delta U)^3/L$ may be developed for comparison [19,30]. Here $\alpha = 1/2$ is a typical hydrodynamic value of the leading constant [31], δU is a typical turbulence speed, and L is a similarity length scale describing the energy-containing structures. If we adopt $L \approx 250 d_e$ and conservatively estimate the turbulence amplitude using the magnetic fluctuation energy, leading to the estimate $\epsilon \approx (\delta V_A^3/L) = 1.3 \times 10^{-9} c^3/d_e$. This agrees reasonably well with the computed $\Delta E/\Delta t$. The total dissipation of fluid energy may also be estimated as the global (adjusted) work on particles, $\epsilon_e = \langle D_e \rangle = 0.58 \times 10^{-9} c^3/d_e$. It is evident that the highly fluctuating and spatially structured dissipation can account for a substantial part of the measured dissipation, and is in agreement with expectations of a cascade theory.

Finally, we examine intermittency properties of the magnetic field increments [27,32]. Figure 4 shows the scale dependent kurtosis of the increments, both from the filtered data and the unfiltered data. The kurtosis of the filtered signal grows from the mildly non-Gaussian value of ~4 at scales just larger than d_i to more non-Gaussian values ~10.5 near the electron scales $\sim d_e$. Due to filtering at $r = 0.2 d_e$, the values of kurtosis saturate at smaller scales. This behavior of the increments clearly signifies the phenomenon of statistical intermittency of the magnetic field. Numerical experiments conclusively indicate that the kurtosis of the unfiltered signal, which re-Gaussianizes at small scales, is influenced nonlocally in scale by the statistical noise due to finite particle number. This affects the kurtosis and higher order statistics, but not the spectrum.

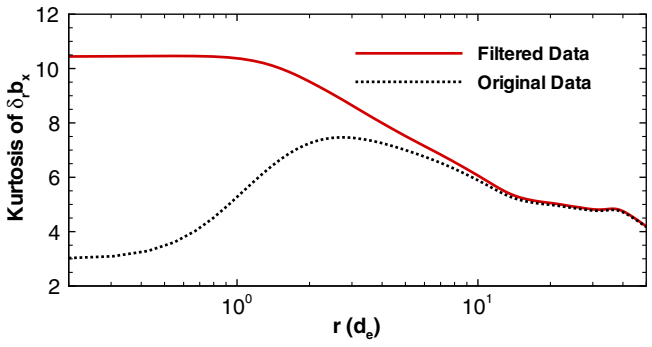

FIG. 4 (color online). Kurtosis of the magnetic field increments $\delta b_x = b_x(y + r) - b_x(y)$ as a function of separation length r, computed with unfiltered data, and data low pass filtered at $kd_e = 5$. The effects of counting statistics at very high k influence kurtosis at much larger scales, between d_e and d_i. In all diagnostics, the results are improved by using the filtered data.

In conclusion, we have studied the nonlinear, turbulent behavior of a kinetic plasma driven by shear using high resolution simulations [10], which show that the strong cascade is characterized by generation of highly structured and filamentary current sheets. The hierarchy extends fully through the range of scale between proton and electron inertial scales. Direct computation of the work done by the electromagnetic field on the particles shows that dissipation occurs nonuniformly, and, in fact, is strongly associated with the strength of the magnetic structures. This microscopic assessment of dissipation agrees well with global energy decay. We conclude that for plasma turbulence originating in planar laminar shear flows, heating and dissipation are highly nonuniform. Many of these properties appear to be consistent with observations of solar wind turbulence at kinetic scales [4,24,25]. These results suggest that nonuniform dissipation in structures extending down to electron scales are likely sources of substantial heating in collisionless space plasmas, consistent with the analysis of magnetosheath observations [33], and analysis of solar wind inertial range statistics [28]. It is, of course, desirable to verify the present 2D analysis in three dimensions and to explore a range of plasma β of relevance to the corona and solar wind; this is addressed in Ref. [10]. Further study of the intermittency properties at kinetic scales will be reported in a subsequent paper, while similar analysis of solar wind data would appear to be a desirable next step.

This research supported in part by NSF Grants No. AGS-1063439 and No. AGS-1156094 (SHINE), and by NASA Grants No. NNX09AG31G and No. NNX11AJ44G (Heliophysics Theory), and by the Solar Probe Plus ISIS project and the Magnetosphere Multiscale Theory and Modeling Program. H. K., V. R., W. D., and B. L. acknowledge support from NASA through the Heliophysics Theory Program and NSF through ATM 0802380 and EAGER 1105084. S. C. C. acknowledges support from the UK STFC. Simulations presented here were performed on resources of the National Center for Computational Sciences at Oak Ridge National Laboratory (Jaguar/Lens), which is supported by DOE under Contract No. DE-AC05-00OR22725.

[1] L. Matteini, P. Hellinger, S. Landi, P. M. Trávníček, and M. Velli, Space Sci. Rev. (in press).
[2] B. A. Maruca, J. C. Kasper, and S. D. Bale, Phys. Rev. Lett. **107**, 201101 (2011).
[3] S. P. Gary and J. E. Borovsky, J. Geophys. Res. **109**, A06105 (2004).
[4] S. D. Bale, P. J. Kellogg, F. S. Mozer, T. S. Horbury, and H. Reme, Phys. Rev. Lett. **94**, 215002 (2005).
[5] S. R. Cranmer, Space Sci. Rev. **101**, 229 (2002).
[6] R. J. Leamon, W. H. Matthaeus, C. W. Smith, and H. K. Wong, Astrophys. J. **507**, L181 (1998).
[7] B. J. Vasquez, C. W. Smith, K. Hamilton, B. T. MacBride, and R. J. Leamon, J. Geophys. Res. **112**, 7101 (2007).
[8] P. D. Mininni, Phys. Rev. E **76**, 026316 (2007).
[9] P. D. Mininni, A. Alexakis, and A. Pouquet, Phys. Rev. E **77**, 036306 (2008).
[10] H. Karimabadi, V. Roytershteyn, M. Wan, W. H. Matthaeus, W. Daughton, P. Wu, M. Shay, B. Loring, J. Borovsky, E. Leonardis, S. Chapman, and T. K. M. Nakamura, Phys. Plasmas (to be published).
[11] W. H. Matthaeus and D. Montgomery, Ann. N.Y. Acad. Sci. **357**, 203 (1980).
[12] V. Carbone, P. Veltri, and A. Mangeney, Phys. Fluids A **2**, 1487 (1990).
[13] D. Biskamp, *Magnetohydrodynamic Turbulence* (Cambridge University Press, Cambridge, England, 2003).
[14] F. Sahraoui, M. L. Goldstein, G. Belmont, P. Canu and L. Rezeau, Phys. Rev. Lett. **105**, 131101 (2010).
[15] S. P. Gary, O. Chang, and J. Wang, Astrophys. J. **755**, L142 (2012).
[16] A. N. Kolmogorov, J. Fluid Mech. **13**, 82 (1962).
[17] A. M. Oboukhov, J. Fluid Mech. **13**, 77 (1962).
[18] J. D. Richardson, K. I. Paularena, A. J. Lazarus, and J. W. Belcher, Geophys. Res. Lett. **22**, 325 (1995).
[19] G. P. Zank, W. H. Matthaeus, and C. W. Smith, J. Geophys. Res. **101**, 17093 (1996).
[20] M. K. Verma, D. A. Roberts, and M. L. Goldstein, J. Geophys. Res. **100**, 19839 (1995).
[21] H. Politano and A. Pouquet, Geophys. Res. Lett. **25**, 273 (1998).
[22] K. T. Osman, M. Wan, W. H. Matthaeus, J. M. Weygand, and S. Dasso, Phys. Rev. Lett. **107**, 165001 (2011).
[23] K. J. Bowers, B. J. Albright, L. Yin, B. Bergen, and T. J. T. Kwan, Phys. Plasmas **15**, 7 (2008).
[24] F. Sahraoui, M. L. Goldstein, P. Robert, and Y. V. Khotyaintsev, Phys. Rev. Lett. **102**, 231102 (2009).
[25] O. Alexandrova, V. Carbone, P. Veltri, and L. Sorriso-Valvo, Astrophys. J. **674**, 1153 (2008).
[26] C. W. Smith, K. Hamilton, B. J. Vasquez, and R. J. Leamon, Astrophys. J. **645**, L85 (2006).
[27] A. S. Monin and A. M. Yaglom, *Statistical Fluid Mechanics* (MIT Press, Cambridge, MA, 1975), Vol. 1–2.
[28] K. T. Osman, W. H. Matthaeus, A. Greco, and S. Servidio, Astrophys. J. Lett. **727**, L11 (2011); K. T. Osman, W. H. Matthaeus, B. Hnat, and S. C. Chapman, Phys. Rev. Lett. **108**, 261103 (2012).
[29] S. Zenitani, M. Hesse, A. Klimas, and M. Kuznetsova, Phys. Rev. Lett. **106**, 195003 (2011).
[30] T. de Kármán and L. Howarth, Proc. R. Soc. Edinburgh, Sect. A **164**, 192 (1938).
[31] B. R. Pearson, P.-A. Krogstad, and W. van de Water, Phys. Fluids **14**, 1288 (2002).
[32] F. Anselmet, Y. Gagne, E. J. Hopfinger, and R. A. Antonia, J. Fluid Mech. **140**, 63 (1984).
[33] D. Sundkvist, A. Retino, A. Vaivads, and S. D. Bale, Phys. Rev. Lett. **99**, 025004 (2007).